ACS APPLIED MATERIALS & INTERFACES

www.acsami.org

Research Article

Facile Patterning of Silver Nanowires with Controlled Polarities via Inkjet-Assisted Manipulation of Interface Adhesion

Tao Wan,* Peiyuan Guan, Xinwei Guan, Long Hu, Tom Wu, Claudio Cazorla, and Dewei Chu

Cite This: *ACS Appl. Mater. Interfaces* 2020, 12, 34086–34094

Read Online

ACCESS | Metrics & More | Article Recommendations | Supporting Information

ABSTRACT: Facile patterning technologies of silver nanowires (AgNWs) with low-cost, high-resolution, designable, scalable, substrate-independent, and transferable characteristics are highly desired. However, it remains a grand challenge for any material processing method to fulfil all desirable features. Herein, a new patterning method is introduced by combining inkjet printing with adhesion manipulation of substrate interfaces. Both positive and negative patterns (i.e., AgNW grid and rectangular patterns) have been simultaneously achieved, and the pattern polarity can be reversed through adhesion modification with judiciously selected supporting layers. The electrical performance of the AgNW grids depends on the AgNW interlocking structure, manifesting a strong structure−property correlation. High-resolution and complex AgNW patterns with line width and spacing as small as 10 μm have been demonstrated through selective deposition of poly(methyl methacrylate) layers. In addition, customized AgNW patterns, such as logos and words, can be fabricated onto A4-size samples and subsequently transferred to targeted substrates, including Si wafers, a curved glass vial, and a beaker. This reported inkjet-assisted process therefore offers a new effective route to manipulate AgNWs for advanced device applications.

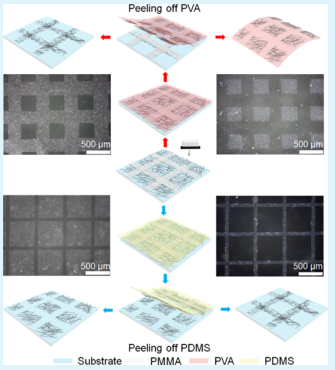

KEYWORDS: *silver nanowires, patterning, polarities, inkjet printing, adhesion manipulation*

1. INTRODUCTION

One-dimensional nanomaterials, such as nanowires, nanotubes, and nanofibers, have attracted tremendous research interest for their potential applications in touch screens,[1,2] flexible displays,[3,4] sensors,[5,6] solar cells,[7,8] and photodetectors.[9,10] Owing to their unique electrical, thermal, optical, and mechanical properties, silver nanowires (AgNWs) have been widely used as building blocks for transparent electronics by patterning or transfer process, enabling device integration and functionalities for next-generation electronic/optoelectronic applications.[1,2,11−13] Despite the rapid development of patterning techniques, an effective AgNW patterning with facile, low-cost, high-resolution, designable, scalable, substrate-independent, and transferable characteristics has yet been reported. Recently, conventional photolithography[14,15] and laser ablation processes[16,17] have been introduced to pattern AgNWs with controlled sizes and shapes, and then an etchant or high-energy laser is generally used to remove the unnecessary parts. However, these patterning methods require expensive equipment and complex processes and suffer from high production costs.[18] As an alternative route, solution-based printing technologies have recently gained great attention in view of their merits of large patterning area, low-cost fabrication, versatile manufacturing, and good compatibility with flexible substrates.[19] A wide range of printing methods have been developed, including inkjet printing,[20,21] screen printing,[22,23] gravure printing,[24,25] and reverse offset printing.[26]

Unlike other printing methods, inkjet printing is a mask- and contact-free approach and has emerged as a promising technique to directly write designed patterns with precise placement on various substrates.[27−30] However, to achieve ultra-fine patterns during the printing process, the ink composition (e.g., concentration, solvent, and other organic additives) needs to be carefully tuned to optimize ink properties (e.g., viscosity and surface tension), hence enabling good stability and printability.[28,31] Apart from complex formulation of inks, the dimension of the materials themselves also affects significantly the printing performance. Great success has been achieved in inkjet printing with quantum dots,[32] nanoparticles,[33] nanosheets,[34] and nanorods,[35] but direct printing of one-dimensional nanomaterials with a high aspect ratio is rather difficult due to the well-known nozzle clogging problem.[20,36,37] While previous studies showed that short AgNWs with length less than 5 μm could be handled by the printing process,[20,38] the overall electrical and optical properties of the printed patterns are severely compromised compared to that from long AgNWs, which are desirable for

Received: April 30, 2020
Accepted: July 9, 2020
Published: July 9, 2020

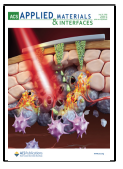

https://dx.doi.org/10.1021/acsami.0c07950
ACS Appl. Mater. Interfaces 2020, 12, 34086−34094

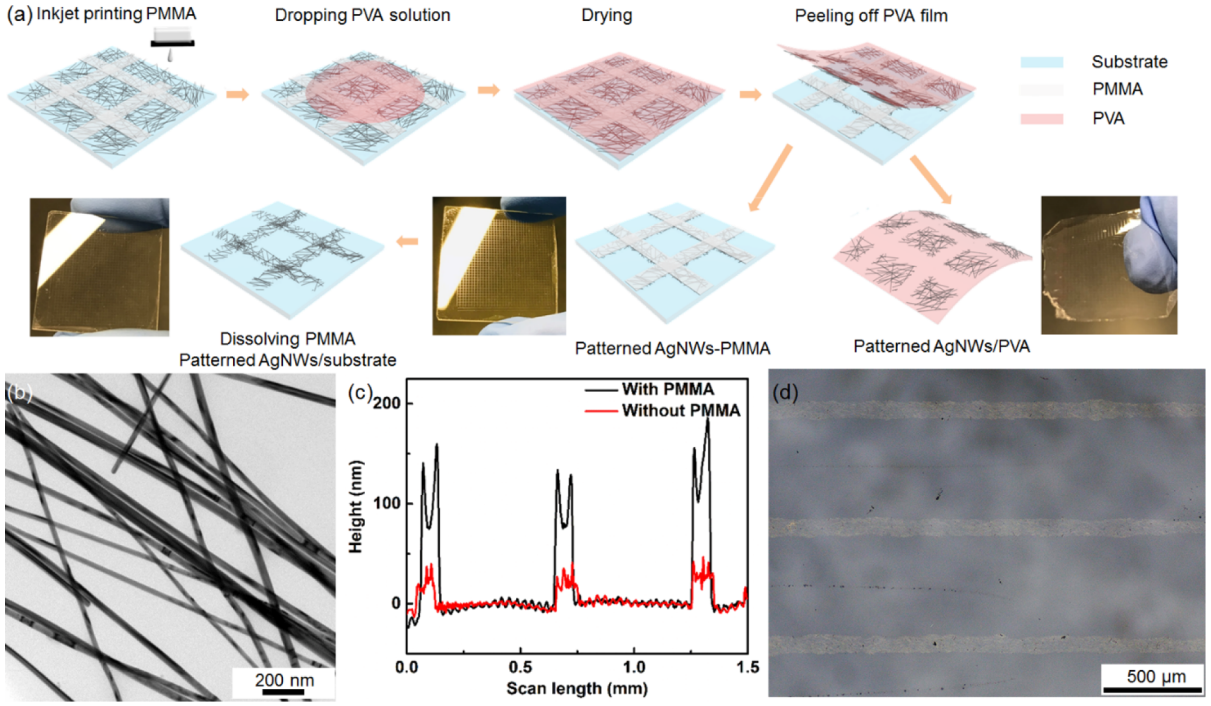

Figure 1. (a) Schematic illustration for the preparation of AgNW patterns by inkjet printing and adhesion manipulation with PVA and related photographs of devices. (b) TEM image of synthesized AgNWs. (c) Thickness of AgNW lines with and without PMMA layer. (d) Bright-field optical image of AgNW lines after dissolving the PMMA layer.

constructing more effective conductive networks through providing longer percolation paths and reducing the nanowire junctions with high contact resistance.[39] This bottleneck of the printing process cannot be overcome via using a bigger nozzle because a poorer pattern resolution is obtained as a result of the nozzle geometry.[28] Although highly ordered NW arrays have been fabricated by incorporating inkjet printing and template-confinement strategy,[40,41] the ordered nanostructure does not provide highly conductive paths for electrode applications.

Another interesting patterning route is to control the interface adhesion between objects and substrates, and a significant advantage of this method is its transferability of patterns onto target substrates, including three-dimensional curved surfaces for curved electronic applications, which cannot be directly printed via conventional printing technology.[42−45] For a AgNW percolation network, the adhesion of AgNWs to underlying substrates relies on their physical adsorption force, which can be modified by changing the surface energy through surface treatments (e.g., UV/O_3 and plasma). The adhesion is selectively controlled with a mask, and AgNWs are either kept or removed, depending on the adhesion force, to form customized shapes.[18,46] Accordingly, the patterning is determined by the applied mask, and low flexibility is expected.

Considering the fact that no single method can simultaneously fulfil all desirable characteristics for practical applications, we introduce herein a facile AgNW patterning method that combines inkjet printing with adhesion manipulation. Instead of printing AgNW ink, we choose a simple, removable, and printable organic ink [e.g., poly(methyl methacrylate) (PMMA solution)] to print customized PMMA layers. Two most common polyvinyl alcohol (PVA) and polydimethylsiloxane (PDMS) supporting layers were employed to manipulate the interface adhesion for the fabrication of positive and negative AgNW patterns without an additional etching or wiping process. The positive pattern corresponds to a replica of the inkjet-printed PMMA pattern, and the negative one is the inverted pattern. As the adhesion between PMMA-covered NWs and substrate is larger than that between PMMA-covered AgNWs and PVA, the covered AgNWs remain on the substrate while the uncovered AgNWs are embedded into the PVA film, leading to positive and negative AgNW patterns, respectively. The grid width as well as the rectangular AgNW pattern can be well tuned by modifying the printing parameters. High-resolution AgNW patterns, such as line width and space around 10 μm, which are unattainable with conventional inkjet printing, are also realized by additional printing and transfer processes. On the other hand, when PDMS is attached to the PMMA-covered sample, the adhesion between covered AgNWs and substrate is weaker than that between covered AgNWs and PDMS after addition of water, hence the covered AgNWs are detached from the substrate and transferred to PDMS. Therefore, a reversed polarity pattern is achieved on the original substrate. The formed AgNW pattern on the PDMS can also be coated onto other substrates, indicating its transfer characteristic for diverse applications.

2. RESULTS AND DISCUSSION

Grid structures with interconnected conductive networks possess optimal electrical, optical, and mechanical performances, and they are promising candidates for flexible transparent electrode applications.[47,48] Therefore, AgNW grid structures were fabricated as an example to demonstrate the patterning quality. Previous studies have shown that organic materials can be used as masks to protect objects for patterning process;[15,49] here, printed PMMA patterns are not only used as protective layers, but also to realize selective interface adhesion

https://dx.doi.org/10.1021/acsami.0c07950
ACS Appl. Mater. Interfaces 2020, 12, 34086−34094

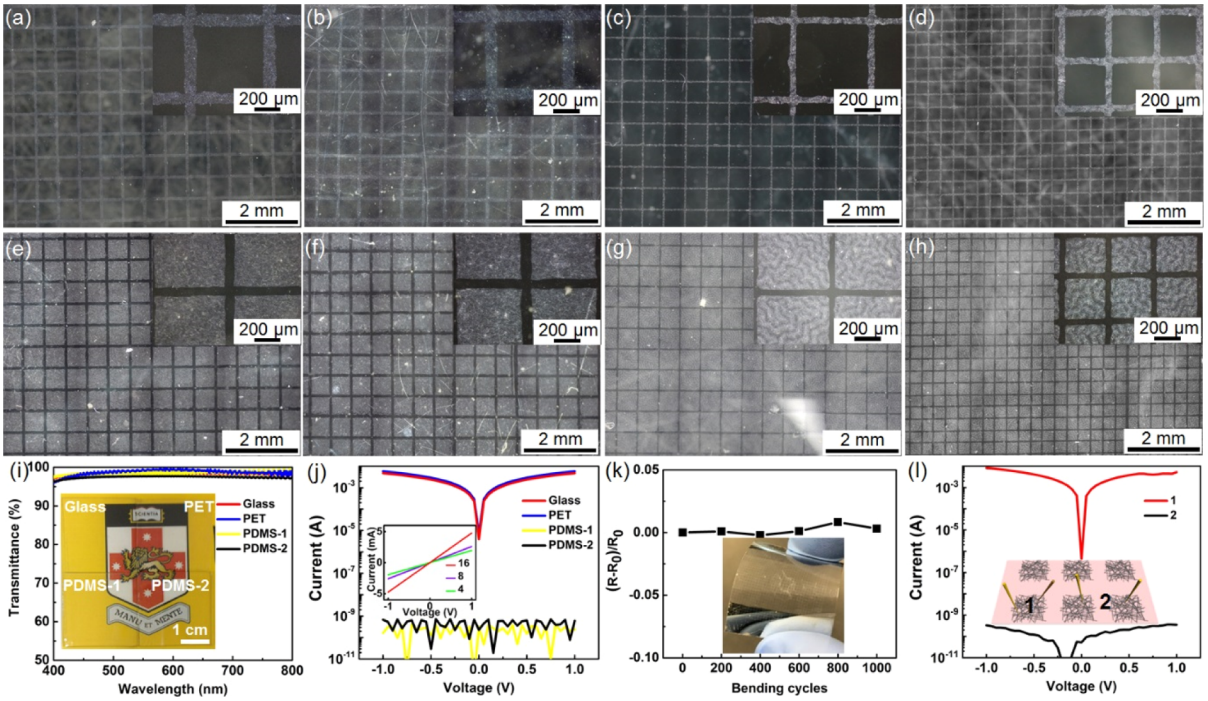

Figure 2. Dark-field optical images of AgNW grids on different substrates: (a) glass, (b) PET, (c) PDMS-1, and (d) PDMS-2. The initial AgNW films are fabricated by spin-coating 16 times. The grid pitch is 600 and 350 μm in (a−c) and (d), respectively. (e−h) Corresponding rectangular arrays on PVA. The insets show the enlarged images of the grids and rectangular shapes. (i) Transmittance spectra of grids on different substrates. The inset shows the corresponding devices. (j) Corresponding $I-V$ curves in log-scale of grids on different substrates. The inset shows the $I-V$ curves in linear scale of the glass samples spin-coated 4, 8, and 16 times. (k) Resistance change of the PET device during bending cycles. The inset shows the flexible PET sample. (l) $I-V$ curves in log-scale of AgNW rectangle and adjacent rectangles on PVA, which is peeled from the glass sample spin-coated 16 times. The inset illustrates the corresponding measurements.

for the fabrication of positive and negative NW patterns. Therefore, the NW pattern resolution is determined by the inkjet-printed PMMA layers. Specifically, PMMA grid structures are fabricated by printing vertical and horizontal PMMA lines sequentially, and positive AgNW grid pattern as well as the corresponding negative AgNW rectangular pattern was easily achieved when PVA film was applied (Figure 1a). As a result, full utilization of the deposited AgNWs is realized during the patterning process and additional etching or wiping process is no longer required, implying simplicity and low-cost of this method. First, PMMA ink (e.g., 6 wt %) is directly printed onto the AgNW film, and then the PVA solution is cast onto the sample surface to form a PVA layer. After drying, the uncovered AgNWs are embedded into the PVA surface, and hence stronger adhesion is formed between AgNWs and PVA compared to that between AgNWs and the original substrate, leading to transfer of AgNWs from the substrate to PVA film during the subsequent peeling off process.[50] However, for the PMMA-covered AgNWs, the printed PMMA not only significantly enhances the adhesion of the AgNWs to the substrate, but also avoids the direct contact between AgNWs and PVA. In this case, the adhesion between covered AgNWs and substrate is stronger than that between covered AgNWs and PVA, so covered AgNWs remain on the substrate, giving rise to selective separation of AgNWs. As a result, a positive grid NW pattern is formed on the original substrate after immersing the PMMA-covered sample in acetone, while negative rectangular AgNW array is moved to the PVA film. The insets in Figure 1a show the photographs of the resulting devices. XRD pattern of AgNWs is shown in Figure S1a, and the five typical diffraction peaks of silver (JCPDS card no. 04-0783) correspond to the (111), (200), (220), (311), and (222) planes. The small peak at 31.8° is assigned to Ag(Cl,Br).[51] Figure 1b shows the TEM image of the synthesized thin AgNWs, and the periodic lattice fringes with a distance of 0.24 nm correspond to the Ag(111) planes (Figure S1b). The average diameter and length of the AgNWs were 39.6 nm and 52.3 μm, respectively (Figure S2).

Figure 1c illustrates the thickness of the obtained AgNW lines with and without PMMA layers. Compared with the AgNW pattern, the much higher thickness of lines with PMMA suggests full protection of the AgNWs, which is necessary for the subsequent patterning process. Given that PMMA concentration greatly affects film thickness as well as printing process, we have changed PMMA concentration for inkjet printing. When a higher concentration (8 wt %) is used, nozzle clogging easily occurs. Although 4 wt % PMMA can print patterns, some of the AgNWs are detached due to discontinuous coverage (Figure S3). Therefore, 6 wt % PMMA solution is employed for the printing process. Figure 1d shows the obtained AgNW lines after removing PMMA layers.

One key advantage of this inkjet-assisted method is its substrate-independent characteristic, which enables PMMA layers to be printed onto different substrates, such as glass, PET, and PDMS (Figure 2a−d). Under the same printing condition, the grid width on glass and PET is about 70−100 μm, while the width on PDMS is about 40−60 μm owing to their different surface wettability (Figure S4).[52] To enable AgNW deposition onto PDMS substrates during sample preparation, UV/O_3 treatment was conducted to change the PDMS surface from intrinsically hydrophobic to hydrophilic,

https://dx.doi.org/10.1021/acsami.0c07950
ACS Appl. Mater. Interfaces 2020, 12, 34086−34094

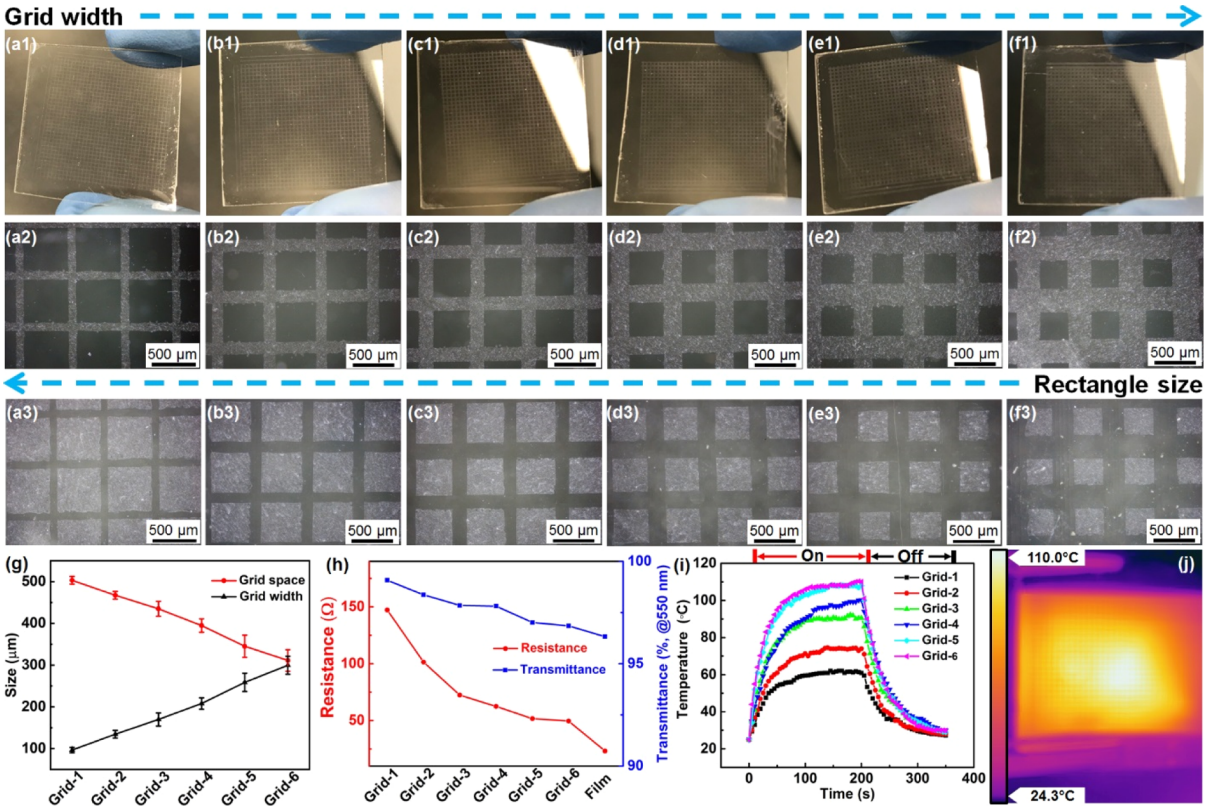

Figure 3. (a1–f1) Photographs of AgNW grid samples with different widths, which are termed Grid-1, Grid-2, Grid-3, Grid-4, Grid-5, and Grid-6, respectively. Dark-field optical images of the corresponding (a2–f2) AgNW grids on glasses and (a3–f3) rectangular arrays on PVA. (g) Average grid width and space of different grid samples. (h) Resistance and transparency at 550 nm of grid samples and initial AgNW film. (i) Temperature profiles of grid samples under applied voltage of 10 V. (j) IR image of Grid-6 at applied voltage of 10 V.

but its hydrophobicity can be recovered over time, leading to a higher contact angle and smaller grid width.[53] In the meantime, the corresponding negative AgNW rectangular patterns are successfully transferred onto PVA films (Figure 2e–h). All grid samples present a high transmittance of above 97% at 550 nm (excluding the substrate) (Figure 2i), demonstrating excellent optical performance. The grids on glass and PET exhibit similar resistance of ~several hundred ohms, but both the PDMS samples with grid pitch of 600 and 350 μm are insulating (Figure 2j), which is ascribed to the different AgNW interlocking structure (Figure S5). After UV/O_3 treatment, the smooth surface of PDMS becomes wrinkled, accordingly resulting in the wrinkled AgNW distribution when AgNWs are spin-coated onto the modified surface (Figure S5d,e). Specifically, dense and sparse AgNWs are periodically distributed in the prepared patterns (Figure S5f), and high resistance is expected because the overall electrical performance of the devices is determined by the numerous sparse regions with high resistance. Besides, the smaller grid width in PDMS samples can also increase its overall resistance. The results clearly reveal that this patterning is not only suitable for flat surface (e.g., glass and PET) but also for coarse surfaces (e.g., wrinkled PDMS). The AgNW density of the samples is tuned by varying the spin-coating times, and the samples with lower AgNW density exhibit a higher resistance, as expected (Figure 2j).

To explore the potential applications in the flexible devices, the flexibility of the PET device is measured by attaching and detaching the sample on a glass vial with a radius of 6 mm for 1000 cycles, and the conductivity of the device remains highly stable during the bending test (Figure 2k). The electrical property of the rectangular array on PVA is also investigated. Conductive and insulating characteristics are clearly observed in the AgNW rectangle and adjacent rectangles, respectively, further confirming the effectivity of the AgNW patterning. Similarly, the prepared AgNW grid pattern can further be transferred to a PVA film by repeating the aforementioned procedures, as shown in Figure S6. We also replace the PVA solution with a PDMS precursor; however, most of the AgNWs are still retained on the original substrate (Figure S7a), and only partial AgNWs are successfully moved to PDMS (Figure S7b), implying that the formed adhesion caused by the solidified PDMS precursor is not enough for the AgNW transfer.

In addition, to further demonstrate the tunability of AgNW patterning and related physical properties of this method, AgNW film with a series of grid width/spacing are fabricated under the same experimental condition. The grids with controllable width and space are fabricated by varying the PMMA line width, and the grid pitch is fixed at 600 μm during ink-jet printing. Figure 3a1–f1 shows the photographs of samples with various grid widths, where grid morphologies and related structure change can be clearly observed. Figure 3a2–f2 present the corresponding optical images, and the average width is gradually increased from ~96 to ~300 μm, while the average grid space is decreased from 503 to ~311 μm (Figure 3g), which is consistent with the given grid pitch. Rectangular AgNW arrays on PVA with tunable size are also obtained, as shown in Figure 3a3–f3.

https://dx.doi.org/10.1021/acsami.0c07950
ACS Appl. Mater. Interfaces 2020, 12, 34086–34094

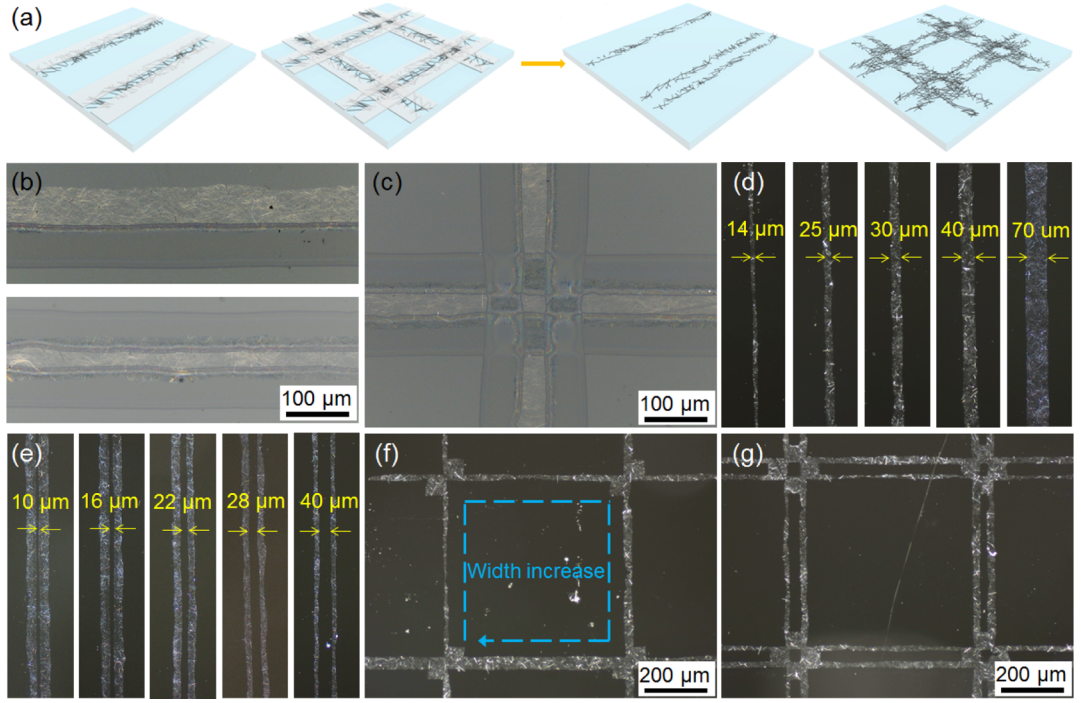

Figure 4. (a) Schematic illustration for the preparation of high-resolution AgNW patterns based on initial patterns. (b,c) Bright-field optical images of AgNW patterns with selectively deposited PMMA layers. (d) Dark-field optical images of AgNWs with different line widths from about 14 to 70 μm. (e) Dark-field optical images of AgNW lines with different gaps from about 10 to 40 μm. (f,g) Dark-field optical images of complex AgNW patterns. The inserted arrow indicates that the grid width increases clockwise.

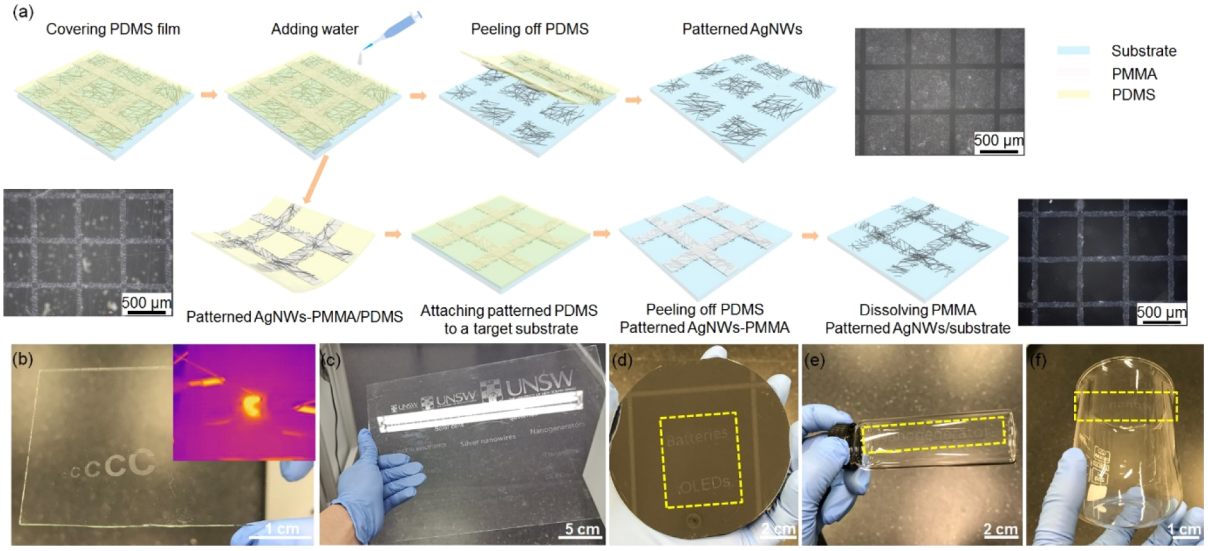

Figure 5. (a) Schematic illustration for the preparation of AgNW patterns with reversed polarity by inkjet printing and adhesion manipulation with PDMS and related optical images are inserted. (b) Letter "C" transferred onto the glass substrate. The inset corresponds to IR image of the letter "C" under 10 V. (c) Designed AgNW pattern with PMMA on an A4-size glass substrate after peeling off the PVA. (d–f) AgNW words from the A4-size glass transferred to Si substrate, a glass vial, and a glass beaker, respectively (indicated by the yellow rectangles). The PMMA layer is removed with acetone.

Figure 3h shows resistance and transmittance at 550 nm of grid samples and initial AgNW network film. It is well known that there exists a trade-off between electrical conductivity and optical transmittance in AgNW interlocking networks.[54] With increasing the grid width, the overall resistance and transparency are gradually decreased from 147 to 50 Ω and 99 to 96.8%, respectively, suggesting that the properties of AgNW samples strongly depend on their structure and can be facilely tailored. Compared with the initial intact film, the grid samples show a higher transmittance because of the higher optical transmission offered from the voids in the grid pattern. However, the voids have an inverse effect on the electrical conductivity, and the samples with a smaller line width exhibit a higher resistivity as less conductive paths are formed due to lower amount of AgNWs.[48] The joule heating performance of these grid samples is studied, and Figure 3i shows their temperature profiles under 10 V. Generally, Joule's law ($P = V^2/R$, where P is the supplied power, V is the applied voltage,

https://dx.doi.org/10.1021/acsami.0c07950
ACS Appl. Mater. Interfaces 2020, 12, 34086−34094

and R is the resistance of the sample) is employed to describe the generated heat.[55] Accordingly, the higher surface temperature is generated in the sample with the bigger grid width due to the lower resistance, and a maximum temperature of ∼110 °C is achieved. The patterned grid structure can also be observed in the infrared (IR) image (Figure 3j).

One major drawback of the inkjet printing technology is its coarse resolution, which impedes its wide application. Generally, the resolution is measured by the line width and space between the lines, and high resolution (<20 μm) can be reached by wettability manipulation through limiting ink spreading.[28,56] On the other hand, as the printer is connected with a computer, accurate location of the droplets on substrates is achievable by moving the nozzle over the desired place,[57] allowing precise deposition of PMMA layers. This process is similar to selective laser ablation and can be utilized to realize high-resolution patterning. Hence, the preformed patterns, such as line and grid structure, are processed for further modification. Specifically, PMMA ink is printed to selectively cover the preformed AgNW pattern, and the covered AgNWs with tunable size will remain on the substrate after the peeling process, leading to customized patterns with high resolution. The schematic illustration is presented in Figure 4a, and related optical images of PMMA-covered AgNW patterns are shown in Figure 4b,c. By controlling the PMMA layer position, the AgNW width can be readily tuned from 70 to about 10 μm (Figure 4d). In addition, to realize narrowly separated thin AgNW patterns, two PMMA lines are deposited on the AgNW pattern, and the gap between AgNW lines is well controlled between 10 and 40 μm by changing the distance between deposited PMMA layers (Figure 4e). In addition to simple line structures with different width and space, complex patterns are fabricated based on the grid structures when single or two separated PMMA lines are printed onto each AgNW line in the grid sample, and other interesting shapes can also be expected with different preformed patterns, revealing excellent flexibility in pattern engineering (Figure 4f,g).

Although the aforementioned PDMS precursor is not suitable for the AgNW patterning, the solidified PDMS film can be used to replace the PVA film as the supporting layer, and interestingly, patterns with reversed polarities are obtained, as shown in Figure 5a. When the PDMS film is firmly attached in the PMMA-patterned sample, a small amount of water (10−20 μL) is dropped onto one edge of the sample, and water penetrates because of wettability contrast between the substrate and PMMA-covered AgNWs,[58] which favors the separation of covered NWs from the initial substrate. In this case, the adhesion between covered AgNWs and glass is weaker than that between covered AgNWs and PDMS, which is contrary to the results with PVA and favors the transfer of the positive pattern to the PDMS. Therefore, the negative rectangular pattern is left on the original substrate. The positive AgNW pattern on the PDMS is then transferred to target substrates by wrapping the PDMS around the substrates. To enable this transfer process, a heating treatment is required to detach the covered AgNWs from PDMS by reducing the interface adhesion.[59] Figure 5b shows the transferred letters "C" with different font sizes, and the "C" can be clearly seen in the IR image when a voltage is applied using the probes, which suggests the conductive characteristic. To further demonstrate potential applications, a complex pattern, such as University of New South Wales (UNSW) logo, is printed on the PET substrate (Figure S8). Moreover, a designed pattern (Figure S9), including UNSW logos and words, is printed onto the A4-size AgNW sample (Figure 5c). The peeled PVA film is shown in Figure S10. Apart from the common glass substrate, the word patterns ("Batteries" and "OLEDs") are also transferred to a Si substrate (Figure 5d). Furthermore, the word patterns ("Nanogenerators" and "Silver nanowires") are successfully transferred to a curved glass vial and a beaker, respectively (Figure 5e,f). The words "Silver nanowires" with PMMA layer are obviously observed before the final transfer process, as shown in Figure S11.

3. CONCLUSIONS

In conclusion, we developed a straightforward method to fabricate complex AgNW patterns by combining inkjet printing and adhesion manipulation. PMMA ink was first printed onto NWs to form customized PMMA patterns, which were utilized as templates for the NW transfer process with PVA and PDMS layers. By selectively controlling the interface adhesion between PMMA-covered AgNWs and different supporting layers, AgNW patterns with different polarities (e.g., AgNW grid and rectangular patterns) could be facilely achieved, and the patterns with tunable size were also demonstrated, leading to different electrical performances. In addition, high-resolution patterns, such as line width and space around 10 μm, were successfully generated through selectively peeling the AgNWs from the preformed patterns. The inkjet-assisted method enables the preparation of customized AgNW patterns with complex shapes on a large area substrate and could further be transferred to other target substrates, which has tremendous application prospects in device fabrication and engineering.

4. EXPERIMENTAL SECTION

4.1. Sample Preparation. AgNWs were prepared by a modified solvothermal process,[60] and 150 μL of NaCl and NaBr solution was added to synthesize thinner AgNWs (aspect ratio ∼ 1300). The synthesized Ag NWs were dispersed in ethanol with a concentration of ∼0.25 mg/mL. Precleaned glass and PET (2.5 cm × 2.5 cm) were used as substrates. In addition, a PDMS precursor (10:1 weight ratio of the base and curing agent, Sylgard 184, Dow Corning) was spin-coated onto the precleaned glass (800 rpm for 10 s and then 3000 rpm for 30 s).[33] It was further annealed in a preheated oven at 80 °C for 1 h to fabricate the PDMS-based substrate. The PDMS substrates were treated by UV/ozone radiation for 30 min before AgNW deposition. Then, 100 μL of AgNWs were dropped onto the substrates with an initial waiting time of 60 s before the spin-coating process at a speed of 1000 rpm for 15 s. Different AgNW densities were prepared by repeating spin-coating 4, 8, and 16 times, and the corresponding areal mass densities were 7.7, 12.5, and 15.2 mg m^{-2}, which were measured using ImageJ software.[61] PMMA (Sigma-Aldrich) solution was prepared by dissolving PMMA into anisole (Sigma-Aldrich), and the concentration of the ink was 4, 6, and 8 wt %. An inkjet printer (DMP-2800, Fujifilm Dimatix) with a 10 pl cartridge was used to print the PMMA patterns, and 2 mL of the ink was filled into the cartridge. During the printing process, one nozzle was employed. The jetting voltage was set between 25 and 35 V, and the used frequency was 23 kHz. After printing, the samples with PMMA patterns were annealed in the preheated oven at 80 °C for 1 h. Two different methods have been subsequently used to fabricate AgNW patterns by adhesion manipulation.

(1) PVA: 0.5 mL of 10 wt % PVA aqueous solution was used and fully covered the printed samples. After drying at room temperature, the PVA film was peeled from the substrate, and the negative pattern was obtained on the PVA film. The positive pattern on the original substrate was prepared after the PMMA protective layer was removed with acetone.

https://dx.doi.org/10.1021/acsami.0c07950
ACS Appl. Mater. Interfaces 2020, 12, 34086−34094

(2) PDMS: Thin PDMS films were prepared by curing the aforementioned PDMS precursor in a preheated oven at 80 °C for 1 h; then it was firmly attached to the aforementioned PMMA-patterned samples. Water (10−20 μL) was dropped at one edge of the samples with PDMS. After slowly peeling off the PDMS, the positive pattern with PMMA layer was moved to the PDMS film and the negative pattern remained on the original substrate. Afterward, the pattern on the PDMS film was wrapped around the preheated target substrates (70−90 °C) for 10 min to allow the transfer process. Similarly, the positive AgNW pattern was finally attained after dissolving the PMMA layer with acetone.

To fabricate high-resolution patterns, the aforementioned lines and grids were further modified with inkjet printing, and PMMA ink was printed to partly cover the preformed AgNW lines. Accordingly, the PMMA-covered NWs remained on the substrate after the peeling process, and NW line patterns with different width were achieved by carefully controlling the PMMA position. AgNW lines with tunable gap were also prepared when two separated PMMA lines were selectively deposited onto the preformed NW lines. Similarly, single or two separated PMMA lines can be printed onto each AgNW line in the NW grid to fabricate complex structures with thin AgNW lines.

Additionally, the A4-size AgNW film was fabricated by a slot-die method. After the customized pattern was printed, PVA aqueous solution was dropped onto the film and then peeled off after being dried. The patterned words on the substrate were wrapped onto different substrates, including Si, a glass vial, and a beaker, for the pattern transfer, and different Ag patterns were obtained after the PMMA layer was washed with acetone.

4.2. Characterizations. The AgNW morphology was observed with optical microscopy (Olympus BX53 Microscope) and transmission electron microscopy (TEM, Phillips CM 200). The structural characterization of Ag NWs was measured using X-ray diffraction (XRD, PANalytical Empyrean Thin-Film) with Cu K_α radiation. The thickness of the samples was measured by a D-600 Stylus Profiler (KLA-Tencor). The contact angles of the PMMA solution on the substrates were measured with a Data physics OCA-20 system. The transmittances of the samples were acquired by a PerkinElmer ultraviolet−visible (UV−vis) spectrometer. The electrical properties of the grid samples were measured using a Keithley 4200 Semiconductor Characterization System. Two parallel silver electrodes with a thickness of 50 nm were deposited by a sputter coater (Leica EM ACE 600) to improve the contact, and the samples were clamped by two features connected to the Keithley 4200. The distance between the electrodes was 1.5 cm, and the length of NW lines was 2 cm. The surface temperature and thermal images were obtained with an infrared camera (FLIR ONE), and a Keysight b2902a source meter was used to apply the voltage. For heating behavior of the letter "C", conductive Ag electrodes were printed onto the two edges of the letter by the inkjet printer with conductive silver printing ink (Sigma-Aldrich, 30−35 wt % in triethylene glycol monomethyl ether) and dried at 100 °C for 30 min to improve the contact between the probes.

■ ASSOCIATED CONTENT

Supporting Information

The Supporting Information is available free of charge at https://pubs.acs.org/doi/10.1021/acsami.0c07950.

XRD and high-resolution TEM of the Ag NWs; diameter and length histograms of the AgNWs; image of AgNW pattern with 4% PMMA solution; contact angle of PMMA solution on different substrate; images of AgNWs and patterns; image of AgNW pattern transferred to PVA; images of PMMA-covered AgNWs after PDMS peeling off and AgNWs transferred to PDMS; photograph of PMMA-covered AgNWs with UNSW logo; image of the designed pattern; photograph of the PVA film peeled from the A4-size AgNW sample; and words on PDMS transferred from the A4-size glass (PDF)

■ AUTHOR INFORMATION

Corresponding Author

Tao Wan − *School of Materials Science and Engineering, The University of New South Wales (UNSW), Sydney, New South Wales 2052, Australia;* orcid.org/0000-0001-9345-8624; Email: tao.wan@unsw.edu.au

Authors

Peiyuan Guan − *School of Materials Science and Engineering, The University of New South Wales (UNSW), Sydney, New South Wales 2052, Australia*

Xinwei Guan − *School of Materials Science and Engineering, The University of New South Wales (UNSW), Sydney, New South Wales 2052, Australia*

Long Hu − *School of Materials Science and Engineering, The University of New South Wales (UNSW), Sydney, New South Wales 2052, Australia*

Tom Wu − *School of Materials Science and Engineering, The University of New South Wales (UNSW), Sydney, New South Wales 2052, Australia;* orcid.org/0000-0003-0845-4827

Claudio Cazorla − *School of Materials Science and Engineering, The University of New South Wales (UNSW), Sydney, New South Wales 2052, Australia;* orcid.org/0000-0002-6501-4513

Dewei Chu − *School of Materials Science and Engineering, The University of New South Wales (UNSW), Sydney, New South Wales 2052, Australia;* orcid.org/0000-0003-4581-0560

Complete contact information is available at: https://pubs.acs.org/10.1021/acsami.0c07950

Notes

The authors declare no competing financial interest.

■ ACKNOWLEDGMENTS

This work was supported by the Australian Research Council Project of LP190100829.

■ REFERENCES

(1) Cho, S.; Kang, S.; Pandya, A.; Shanker, R.; Khan, Z.; Lee, Y.; Park, J.; Craig, S. L.; Ko, H. Large-Area Cross-Aligned Silver Nanowire Electrodes for Flexible, Transparent, and Force-Sensitive Mechanochromic Touch Screens. *ACS Nano* **2017**, *11*, 4346−4357.

(2) Sannicolo, T.; Lagrange, M.; Cabos, A.; Celle, C.; Simonato, J.-P.; Bellet, D. Metallic Nanowire-based Transparent Electrodes for Next Generation Flexible Devices: a Review. *Small* **2016**, *12*, 6052−6075.

(3) Liu, Z.; Xu, J.; Chen, D.; Shen, G. Flexible Electronics based on Inorganic Nanowires. *Chem. Soc. Rev.* **2015**, *44*, 161−192.

(4) Zhao, J.; Chi, Z.; Yang, Z.; Chen, X.; Arnold, M. S.; Zhang, Y.; Xu, J.; Chi, Z.; Aldred, M. P. Recent Developments of Truly Stretchable Thin Film Electronic and Optoelectronic Devices. *Nanoscale* **2018**, *10*, 5764−5792.

(5) Jayathilaka, W. A. D. M.; Qi, K.; Qin, Y.; Chinnappan, A.; Serrano-García, W.; Baskar, C.; Wang, H.; He, J.; Cui, S.; Thomas, S. W.; Ramakrishna, S. Significance of Nanomaterials in Wearables: A Review on Wearable Actuators and Sensors. *Adv. Mater.* **2019**, *31*, 1805921.

(6) Matsuhisa, N.; Chen, X.; Bao, Z.; Someya, T. Materials and Structural Designs of Stretchable Conductors. *Chem. Soc. Rev.* **2019**, *48*, 2946−2966.

(7) Wang, H.-P.; Periyanagounder, D.; Li, A.-C.; He, J.-H. Fabrication of Silicon Hierarchical Structures for Solar Cell Applications. *IEEE Access* **2018**, *7*, 19395−19400.
(8) Das, S.; Hossain, M. J.; Leung, S.-F.; Lenox, A.; Jung, Y.; Davis, K.; He, J.-H.; Roy, T. A Leaf-inspired Photon Management Scheme using Optically Tuned Bilayer Nanoparticles for Ultra-thin and Highly Efficient Photovoltaic Devices. *Nano Energy* **2019**, *58*, 47−56.
(9) Ning, Y.; Zhang, Z.; Teng, F.; Fang, X. Novel Transparent and Self-powered UV Photodetector based on Crossed ZnO Nanofiber Array Homojunction. *Small* **2018**, *14*, 1703754.
(10) Zhang, Z.; Ning, Y.; Fang, X. From Nanofibers to Ordered ZnO/NiO Heterojunction Arrays for Self-powered and Transparent UV Photodetectors. *J. Mater. Chem. C* **2019**, *7*, 223−229.
(11) Chen, Y.; Ding, X.; Steven Lin, S.-C.; Yang, S.; Huang, P.-H.; Nama, N.; Zhao, Y.; Nawaz, A. A.; Guo, F.; Wang, W.; Gu, Y.; Mallouk, T. E.; Huang, T. J. Tunable Nanowire Patterning using Standing Surface Acoustic Waves. *ACS Nano* **2013**, *7*, 3306−3314.
(12) Tseng, J.-Y.; Lee, L.; Huang, Y.-C.; Chang, J.-H.; Su, T.-Y.; Shih, Y.-C.; Lin, H.-W.; Chueh, Y.-L. Pressure Welding of Silver Nanowires Networks at Room Temperature as Transparent Electrodes for Efficient Organic Light-Emitting Diodes. *Small* **2018**, *14*, 1800541.
(13) Le, V.-Q.; Do, T.-H.; Retamal, J. R. D.; Shao, P.-W.; Lai, Y.-H.; Wu, W.-W.; He, J.-H.; Chueh, Y.-L.; Chu, Y.-H. Van Der Waals Heteroepitaxial AZO/NiO/AZO/Muscovite (ANA/Muscovite) Transparent Flexible Memristor. *Nano Energy* **2019**, *56*, 322−329.
(14) Lee, M.-S.; Lee, K.; Kim, S.-Y.; Lee, H.; Park, J.; Choi, K.-H.; Kim, H.-K.; Kim, D.-G.; Lee, D.-Y.; Nam, S.; Park, J.-U. High-performance, Transparent, and Stretchable Electrodes using Graphene−metal Nanowire Hybrid Structures. *Nano Lett.* **2013**, *13*, 2814−2821.
(15) Wu, J.; Que, X.; Hu, Q.; Luo, D.; Liu, T.; Liu, F.; Russell, T. P.; Zhu, R.; Gong, Q. Multi-length Scaled Silver Nanowire Grid for Application in Efficient Organic Solar Cells. *Adv. Funct. Mater.* **2016**, *26*, 4822−4828.
(16) Kim, H.; Lee, H.; Ha, I.; Jung, J.; Won, P.; Cho, H.; Yeo, J.; Hong, S.; Han, S.; Kwon, J.; Cho, K.-J.; Ko, S. H. Biomimetic Color Changing Anisotropic Soft Actuators with Integrated Metal Nanowire Percolation Network Transparent Heaters for Soft Robotics. *Adv. Funct. Mater.* **2018**, *28*, 1801847.
(17) Fang, Y.; Ding, K.; Wu, Z.; Chen, H.; Li, W.; Zhao, S.; Zhang, Y.; Wang, L.; Zhou, J.; Hu, B. Architectural Engineering of Nanowire Network Fine Pattern for 30 μm Wide Flexible Quantum Dot Light-emitting Diode Application. *ACS Nano* **2016**, *10*, 10023−10030.
(18) Ko, D.; Gu, B.; Kang, S. J.; Jo, S.; Hyun, D. C.; Kim, C. S.; Kim, J. Critical Work of Adhesion for Economical Patterning of Silver Nanowire-based Transparent Electrodes. *J. Mater. Chem. A* **2019**, *7*, 14536−14544.
(19) Li, D.; Lai, W.-Y.; Zhang, Y.-Z.; Huang, W. Printable Transparent Conductive Films for Flexible Electronics. *Adv. Mater.* **2018**, *30*, 1704738.
(20) Finn, D. J.; Lotya, M.; Coleman, J. N. Inkjet Printing of Silver Nanowire Networks. *ACS Appl. Mater. Interfaces* **2015**, *7*, 9254−9261.
(21) Choi, K.-H.; Yoo, J.; Lee, C. K.; Lee, S.-Y. All-inkjet-printed, Solid-state Flexible Supercapacitors on Paper. *Energy Environ. Sci.* **2016**, *9*, 2812−2821.
(22) Liang, J.; Tong, K.; Pei, Q. A Water-based Silver-nanowire Screen-print Ink for the Fabrication of Stretchable Conductors and Wearable Thin-film Transistors. *Adv. Mater.* **2016**, *28*, 5986−5996.
(23) Li, D.; Liu, X.; Chen, X.; Lai, W. Y.; Huang, W. A Simple Strategy towards Highly Conductive Silver-nanowire Inks for Screen-Printed Flexible Transparent Conductive Films and Wearable Energy-storage Devices. *Adv. Mater. Technol.* **2019**, *4*, 1900196.
(24) Huang, Q.; Zhu, Y. Gravure Printing of Water-based Silver Nanowire Ink on Plastic Substrate for Flexible Electronics. *Sci. Rep.* **2018**, *8*, 15167.
(25) Scheideler, W. J.; Smith, J.; Deckman, I.; Chung, S.; Arias, A. C.; Subramanian, V. A Robust, Gravure-printed, Silver Nanowire/metal Oxide Hybrid Electrode for High-throughput Patterned Transparent Conductors. *J. Mater. Chem. C* **2016**, *4*, 3248−3255.
(26) Park, K.; Woo, K.; Kim, J.; Lee, D.; Ahn, Y.; Song, D.; Kim, H.; Oh, D.; Kwon, S.; Lee, Y. High-resolution and Large-area Patterning of Highly Conductive Silver Nanowire Electrodes by Reverse Offset Printing and Intense Pulsed Light Irradiation. *ACS Appl. Mater. Interfaces* **2019**, *11*, 14882−14891.
(27) Chung, S.; Cho, K.; Lee, T. Recent Progress in Inkjet-printed Thin-film Transistors. *Adv. Sci.* **2019**, *6*, 1801445.
(28) Wu, L.; Dong, Z.; Li, F.; Zhou, H.; Song, Y. Emerging Progress of Inkjet Technology in Printing Optical Materials. *Adv. Opt. Mater.* **2016**, *4*, 1915−1932.
(29) Alamri, A. M.; Leung, S.; Vaseem, M.; Shamim, A.; He, J.-H. Fully Inkjet-printed Photodetector Using a Graphene/Perovskite/Graphene Heterostructure. *IEEE Trans. Electron Devices* **2019**, *66*, 2657−2661.
(30) Liu, J.; Shabbir, B.; Wang, C.; Wan, T.; Ou, Q.; Yu, P.; Tadich, A.; Jiao, X.; Chu, D.; Qi, D.; Li, D.; Kan, R.; Huang, Y.; Dong, Y.; Jasieniak, J.; Zhang, Y.; Bao, Q. Flexible, Printable Soft-X-Ray Detectors Based on All-Inorganic Perovskite Quantum Dots. *Adv. Mater.* **2019**, *31*, 1901644.
(31) Kim, D.; Ko, Y.; Kwon, G.; Kim, U.-J.; You, J. Micropatterning Silver Nanowire Networks on Cellulose Nanopaper for Transparent Paper Electronics. *ACS Appl. Mater. Interfaces* **2018**, *10*, 38517−38525.
(32) Liu, Y.; Han, F.; Li, F.; Zhao, Y.; Chen, M.; Xu, Z.; Zheng, X.; Hu, H.; Yao, J.; Guo, T.; Lin, W.; Zheng, Y.; You, B.; Liu, P.; Li, Y.; Qian, L. Inkjet-printed Unclonable Quantum Dot Fluorescent Anti-counterfeiting Labels with Artificial Intelligence Authentication. *Nat. Commun.* **2019**, *10*, 2409.
(33) Jiang, J.; Bao, B.; Li, M.; Sun, J.; Zhang, C.; Li, Y.; Li, F.; Yao, X.; Song, Y. Fabrication of Transparent Multilayer Circuits by Inkjet Printing. *Adv. Mater.* **2016**, *28*, 1420−1426.
(34) Kelly, A. G.; Hallam, T.; Backes, C.; Harvey, A.; Esmaeily, A. S.; Godwin, I.; Coelho, J.; Nicolosi, V.; Lauth, J.; Kulkarni, A.; Kinge, S.; Siebbeles, L. D. A.; Duesberg, G. S.; Coleman, J. N. All-printed Thin-film Transistors from Networks of Liquid-exfoliated Nanosheets. *Science* **2017**, *356*, 69−73.
(35) Kang, H.; Lee, G.-H.; Jung, H.; Lee, J. W.; Nam, Y. Inkjet-printed Biofunctional Thermo-plasmonic Interfaces for Patterned Neuromodulation. *ACS Nano* **2018**, *12*, 1128−1138.
(36) Cui, Z.; Han, Y.; Huang, Q.; Dong, J.; Zhu, Y. Electrohydrodynamic Printing of Silver Nanowires for Flexible and Stretchable Electronics. *Nanoscale* **2018**, *10*, 6806−6811.
(37) Chen, S.-P.; Durán Retamal, J. R.; Lien, D.-H.; He, J.-H.; Liao, Y.-C. Inkjet-printed Transparent Nanowire Thin Film Features for UV Photodetectors. *RSC Adv.* **2015**, *5*, 70707−70712.
(38) Huang, Q.; Al-Milaji, K. N.; Zhao, H. Inkjet Printing of Silver Nanowires for Stretchable Heaters. *ACS Appl. Nano Mater.* **2018**, *1*, 4528−4536.
(39) Jiu, J.; Araki, T.; Wang, J.; Nogi, M.; Sugahara, T.; Nagao, S.; Koga, H.; Suganuma, K.; Nakazawa, E.; Hara, M.; Uchida, H.; Shinozaki, K. Facile Synthesis of Very-long Silver Nanowires for Transparent Electrodes. *J. Mater. Chem. A* **2014**, *2*, 6326−6330.
(40) Lin, C. H.; Kang, C. Y.; Wu, T. Z.; Tsai, C. L.; Sher, C. W.; Guan, X.; Lee, P. T.; Wu, T.; Ho, C. H.; Kuo, H. C.; He, J. H. Giant Optical Anisotropy of Perovskite Nanowire Array Films. *Adv. Funct. Mater.* **2020**, *30*, 1909275.
(41) Lin, C.-H.; Li, T.-Y.; Zhang, J.; Chiao, Z.-Y.; Wei, P.-C.; Fu, H.-C.; Hu, L.; Yu, M.-J.; Ahmed, G. H.; Guan, X.; Ho, C.-H.; Wu, T.; Ooi, B. S.; Mohammed, O. F.; Lu, Y.-J.; Fang, X.; He, J.-H. Designed Growth and Patterning of Perovskite Nanowires for Lasing and Wide Color Gamut Phosphors with Long-term Stability. *Nano Energy* **2020**, *73*, 104801.
(42) Meitl, M. A.; Zhu, Z.-T.; Kumar, V.; Lee, K. J.; Feng, X.; Huang, Y. Y.; Adesida, I.; Nuzzo, R. G.; Rogers, J. A. Transfer Printing by Kinetic Control of Adhesion to an Elastomeric Stamp. *Nat. Mater.* **2006**, *5*, 33−38.

https://dx.doi.org/10.1021/acsami.0c07950
ACS Appl. Mater. Interfaces 2020, 12, 34086−34094

(43) Sim, K.; Chen, S.; Li, Z.; Rao, Z.; Liu, J.; Lu, Y.; Jang, S.; Ershad, F.; Chen, J.; Xiao, J.; Yu, C. Three-dimensional Curvy Electronics Created using Conformal Additive Stamp Printing. *Nat. Electron.* **2019**, *2*, 471−479.
(44) Peng, P.; Wu, K.; Lv, L.; Guo, C. F.; Wu, Z. One-step Selective Adhesive Transfer Printing for Scalable Fabrication of Stretchable Electronics. *Adv. Mater. Technol.* **2018**, *3*, 1700264.
(45) Jeong, J. W.; Yang, S. R.; Hur, Y. H.; Kim, S. W.; Baek, K. M.; Yim, S.; Jang, H.-I.; Park, J. H.; Lee, S. Y.; Park, C.-O. High-resolution Nanotransfer Printing Applicable to Diverse Surfaces via Interface-targeted Adhesion Switching. *Nat. Commun.* **2014**, *5*, 5387.
(46) Liu, G.-S.; Liu, C.; Chen, H.-J.; Cao, W.; Qiu, J.-S.; Shieh, H.-P. D.; Yang, B.-R. Electrically Robust Silver Nanowire Patterns Transferrable onto Various Substrates. *Nanoscale* **2016**, *8*, 5507−5515.
(47) Hu, S.; Gu, J.; Zhao, W.; Ji, H.; Ma, X.; Wei, J.; Li, M. Silver-nanowire Mesh-structured Transparent Conductive Film with Improved Transparent Conductive Properties and Mechanical Performance. *Adv. Mater. Technol.* **2019**, *4*, 1900194.
(48) Lee, H. B.; Jin, W.-Y.; Ovhal, M. M.; Kumar, N.; Kang, J.-W. Flexible Transparent Conducting Electrodes based on Metal Meshes for Organic Optoelectronic Device Applications: a Review. *J. Mater. Chem. C* **2019**, *7*, 1087−1110.
(49) Li, W.; Meredov, A.; Shamim, A. Coat-and-print Patterning of Silver Nanowires for Flexible and Transparent Electronics. *npj Flexible Electron.* **2019**, *3*, 19.
(50) Zeng, X.-Y.; Zhang, Q.-K.; Yu, R.-M.; Lu, C.-Z. A New Transparent Conductor: Silver Nanowire Film Buried at the Surface of a Transparent Polymer. *Adv. Mater.* **2010**, *22*, 4484−4488.
(51) Wan, M.; Tao, J.; Jia, D.; Chu, X.; Li, S.; Ji, S.; Ye, C. High-Purity Very Thin Silver Nanowires Obtained by Ostwald Ripening-driven Coarsening and Sedimentation of Nanoparticles. *CrystEngComm* **2018**, *20*, 2834−2840.
(52) Kuang, M.; Wang, L.; Song, Y. Controllable Printing Droplets for High-resolution Patterns. *Adv. Mater.* **2014**, *26*, 6950−6958.
(53) Cai, L.; Zhang, S.; Miao, J.; Yu, Z.; Wang, C. Fully Printed Stretchable Thin-film Transistors and Integrated Logic Circuits. *ACS Nano* **2016**, *10*, 11459−11468.
(54) Sun, Y.; Chang, M.; Meng, L.; Wan, X.; Gao, H.; Zhang, Y.; Zhao, K.; Sun, Z.; Li, C.; Liu, S.; Wang, H.; Liang, J.; Chen, Y. Flexible Organic Photovoltaics based on Water-Processed Silver Nanowire Electrodes. *Nat. Electron.* **2019**, *2*, 513−520.
(55) Lee, J.-G.; Lee, J.-H.; An, S.; Kim, D.-Y.; Kim, T.-G.; Al-Deyab, S. S.; Yarin, A. L.; Yoon, S. S. Highly Flexible, Stretchable, Wearable, Patternable and Transparent Heaters on Complex 3D Surfaces Formed from Supersonically Sprayed Silver Nanowires. *J. Mater. Chem. A* **2017**, *5*, 6677−6685.
(56) Fukuda, K.; Someya, T. Recent Progress in the Development of Printed Thin-film Transistors and Circuits with High-fesolution Printing Technology. *Adv. Mater.* **2017**, *29*, 1602736.
(57) Derby, B. Inkjet Printing of Functional and Structural Materials: Fluid Property Requirements, Feature Stability, and Resolution. *Annu. Rev. Mater. Res.* **2010**, *40*, 395−414.
(58) Li, H.; Wu, J.; Huang, X.; Yin, Z.; Liu, J.; Zhang, H. A Universal, Rapid Method for Clean Transfer of Nanostructures onto Various Substrates. *ACS Nano* **2014**, *8*, 6563−6570.
(59) Park, J.; Yoon, H.; Kim, G.; Lee, B.; Lee, S.; Jeong, S.; Kim, T.; Seo, J.; Chung, S.; Hong, Y. Highly Customizable All Solution−processed Polymer Light Emitting Diodes with Inkjet Printed Ag and Transfer Printed Conductive Polymer Electrodes. *Adv. Funct. Mater.* **2019**, *29*, 1902412.
(60) Zhu, Y.; Wan, T.; Guan, P.; Wang, Y.; Wu, T.; Han, Z.; Tang, G.; Chu, D. Improving Thermal and Electrical Stability of Silver Nanowire Network Electrodes through Integrating Graphene Oxide Intermediate Layers. *J. Colloid Interface Sci.* **2020**, *566*, 375−382.
(61) Sannicolo, T.; Charvin, N.; Flandin, L.; Kraus, S.; Papanastasiou, D. T.; Celle, C.; Simonato, J.-P.; Muñoz-Rojas, D.; Jiménez, C.; Bellet, D. Electrical Mapping of Silver Nanowire Networks: A Versatile Tool for Imaging Network Homogeneity and Degradation Dynamics during Failure. *ACS Nano* **2018**, *12*, 4648−4659.

https://dx.doi.org/10.1021/acsami.0c07950
ACS Appl. Mater. Interfaces 2020, 12, 34086−34094